Dopamine neurons create Pavlovian conditioned stimuli with circuit-defined motivational properties

Benjamin T. Saunders [ID][1,2,5]*, Jocelyn M. Richard[1,2,5], Elyssa B. Margolis[3] and Patricia H. Janak [ID][1,2,4]*

Environmental cues, through Pavlovian learning, become conditioned stimuli that guide animals toward the acquisition of rewards (for example, food) that are necessary for survival. We tested the fundamental role of midbrain dopamine neurons in conferring predictive and motivational properties to cues, independent of external rewards. We found that brief phasic optogenetic excitation of dopamine neurons, when presented in temporal association with discrete sensory cues, was sufficient to instantiate those cues as conditioned stimuli that subsequently both evoked dopamine neuron activity on their own and elicited cue-locked conditioned behavior. Notably, we identified highly parcelled functions for dopamine neuron subpopulations projecting to different regions of striatum, revealing dissociable dopamine systems for the generation of incentive value and conditioned movement invigoration. Our results indicate that dopamine neurons orchestrate Pavlovian conditioning via functionally heterogeneous, circuit-specific motivational signals to create, gate, and shape cue-controlled behaviors.

The specific contributions of dopamine neurons to learning, motivation, and reinforcement processes, as well as movement, are a longstanding subject of inquiry and debate. This is partially a result of the prominent role of dysfunction in dopamine signaling in both the motivational and motor aberrations that define addiction and Parkinson's disease[1–3], but a major focus of this work is also on dopamine's role in normal Pavlovian cue-reward learning. Manipulation of dopamine neurons can modify the learned value of reward-associated cues (conditioned stimuli, CSs) to alter reward-seeking behavior[4–6] and form contextual preferences[7]. Despite the extensive research history on the subject it remains unknown (i) whether brief, phasic dopamine neuron activity, in the absence of physical reward, can directly assign conditioned properties to discrete sensory cues to make them CSs that elicit conditioned behaviors and (ii) how subpopulations of dopamine neurons[8] may differentially contribute to this process. We addressed this fundamental question using a Pavlovian cue conditioning procedure in which brief optogenetic activation of different groups of dopamine neurons was substituted for natural reward delivery. We found that most dopamine neurons instantiated CS properties in sensory cues, but the motivational value assigned to cues and the corresponding behavioral consequences depended on the specific dopamine circuit that was engaged.

Results

Dopamine neurons imbue environmental cues with CS properties. For selective manipulation of dopamine neurons, we expressed ChR2 in the ventral midbrain in tyrosine hydroxylase (TH)-Cre rats[9], which allowed for optogenetic targeting of TH^{+} dopamine neurons with ~97% specificity (Fig. 1a and Supplementary Fig. 1). To compare the contribution of different dopamine neuronal subpopulations, we implanted optical fibers over ChR2-expressing

dopamine neurons in either the ventral tegmental area (VTA) or substantia nigra pars compacta (SNc) (Fig. 1c,f and Supplementary Fig. 2). To test the contribution of phasic dopamine neuron activity in the creation of conditioned stimuli, we used an optogenetic Pavlovian cue conditioning procedure (Fig. 1b). Rats in paired groups received 25 overlapping cue (light + tone, 7 s) and laser (473 nm; 5 s at 20 Hz, delivered 2 s after cue onset) presentations per session. The cue light was positioned on one wall of the chamber, within rearing height for an adult rat. To control for nonassociative effects of repeated cues and optogenetic stimulation, we exposed separate rats to cue and laser presentations that never overlapped (unpaired groups). VTA and SNc Cre[+] paired groups both quickly learned conditioned responses (CRs), defined here simply as locomotion, during the 7-s cue presentations, and these CRs emerged progressively earlier in the cue period across training for both groups (Fig. 1k and Supplementary Fig. 3). Cre[+] unpaired and Cre[−] controls did not learn CRs (Fig. 1d,g and Supplementary Fig. 3). The latency of CR onset in paired groups decreased across training and, late in training, most CRs were initiated during the first 2 s of each cue period, before laser onset, for both VTA and SNc Cre[+] paired groups (Fig. 1i–k). This indicates that behavior in paired subjects was a conditioned effect, elicited by cue presentations, rather than directly by laser stimulation. Further supporting this, optogenetic activation of dopamine neurons in Cre[+] unpaired groups failed to generate behavior statistically different from Cre[−] controls, during either the cue or laser periods (Fig. 1e,h). These results indicate that, at least for the stimulation parameters that we used, unsignaled phasic midbrain dopamine neuron activity in the VTA or SNc does not reliably act as an unconditioned or conditioned stimulus that can elicit behaviors. We conducted an additional experiment in which rats received cue-laser paired conditioning similar to that described above, but optogenetic stimulation was limited to 1 s per trial

Fig. 1 | Dopamine neurons create Pavlovian conditioned stimuli. a, ChR2 was expressed in TH+ (dopamine) neurons in TH-Cre rats ($n = 40$). **b**, Schematic of optogenetic Pavlovian conditioning task. After habituation to a novel, neutral cue, paired groups received cue and laser (473 nm) presentations that overlapped in time. Unpaired groups received cue and laser presentations separated in time by an average of 80 s. **c**, Targeting ChR2-eYFP to TH+ neurons in the VTA ($n = 22$). **d**, Across training, CRs (locomotion) emerged during the 7-s cue period for VTA Cre+ paired rats ($n = 8$), but not Cre+ unpaired ($n = 8$) or Cre- paired ($n = 6$) controls (P = probability; two-way repeated measures (RM) ANOVA, session×group interaction, $F_{(6,57)} = 11.85$, $P < 0.0001$; post hoc comparisons with unpaired and Cre- groups). **e**, CRs did not emerge in unpaired ($n = 8$) or Cre- controls ($n = 6$) during the 5-s laser period, as compared with Cre+ paired ($n = 8$) rats (two-way RM ANOVA session×group interaction, $F_{(6,57)} = 14.43$, $P < 0.0001$; post hoc comparisons with unpaired and Cre- groups). **f**, Targeting ChR2-eYFP to TH+ neurons in the SNc ($n = 18$). **g**, Cues evoked robust CRs in SNc Cre+ cue-paired ($n = 8$) rats, but not in unpaired ($n = 5$) or Cre- ($n = 5$) controls (two-way RM ANOVA session×group interaction, $F_{(6,48)} = 13.47$, $P < 0.0001$; post hoc comparisons with unpaired and Cre- groups). **h**, CRs did not emerge for SNc Cre+ unpaired ($n = 5$) or Cre- controls ($n = 5$) during the laser period, as compared with Cre+ paired rats (two-way RM ANOVA session×group interaction, $F_{(6,48)} = 12.32$, $P < 0.0001$; post hoc comparisons with unpaired and Cre- groups). **i,j**, For VTA ($n = 8$) and SNc Cre+ ($n = 8$) paired rats, across training, the majority of CRs were initiated in the 2 s after cue onset, but before laser onset (two-way RM ANOVA main effect of session, $F_{(3,42)} = 53.16$, $P < 0.0001$; post hoc comparisons with day 1; **i**), indicating they were cue, rather than laser, evoked. Accordingly, the latency of CR onset for Cre+ paired ($n = 16$) rats decreased across training (two-way RM ANOVA main effect of session $F_{(3,42)} = 27.09$, $P < 0.0001$; post hoc comparisons with day 1; **j**). **k**, On trials in which a CR occurred, the cumulative probability of CR occurrence at each second during the 7-s cue presentations. CRs emerged earlier in the cue period across training for both VTA and SNc Cre+ paired groups. Post hoc comparisons are Bonferroni corrected. Data are expressed as mean ± s.e.m. *$P < 0.05$; ***$P < 0.0001$.

(20 5-ms pulses at 20 Hz, delivered in the final 1 s of cue presentations). Here too, cue-evoked locomotion emerged, with the same probability as seen in the 5-s laser conditioning groups (Supplementary Fig. 4). Together, our results suggest that the contiguous or contemporaneous occurrence of salient sensory cues at the time dopamine neurons are active serves as a critical gate on the ability of dopamine neurons to promote behavior. This provides important context to recent studies on the contribution of dopamine neurons to explicit unconditioned movements[10–12] and, broadly, associative learning.

Dopamine neurons develop phasic increases in population-level activity to dopamine-predictive cues. Cues paired with natural reward evoke phasic activity in dopamine neurons and dopamine release in striatal projection targets[13–16]. Given that we found that optogenetic stimulation of dopamine neurons induced conditioned behavior to discrete paired cues, we asked whether dopamine neurons might acquire phasic neural responses to these paired cues, using fiber photometry[17]. For simultaneous optogenetic stimulation and activity measurement in the same neurons, we co-transfected dopamine neurons with ChrimsonR, a red-shifted excitatory opsin, and the fluorescent calcium indicator GCaMP6f (Fig. 2a,b). This strategy led to a ~90% overlap of GCaMP6 and ChrimsonR expression in TH+ neurons below optic fiber placements in the midbrain (Supplementary Fig. 5a–c). Photoactivation of ChrimsonR (590-nm laser) led to rapid, stable increases in GCaMP6f fluorescence that tightly tracked the length of optogenetic stimulation (Supplementary Fig. 5d). To test the behavioral specificity of light activation of ChrimsonR, we confirmed that 590-nm activation of ChrimsonR-expressing dopamine neurons supported robust intracranial self-stimulation behavior (Supplementary Fig. 5e,f), which rapidly extinguished when the 590-nm laser was switched with a 473-nm laser (Supplementary Fig. 5f). We also recorded photometry signals as rats consumed 100 μl of a 10% sucrose solution. This produced a multi-second calcium fluorescence increase that was similar to that evoked by a 5-s laser train in the same animals (Supplementary Fig. 5g), indicating that, at least at the population level, the optogenetic conditioning procedure taps into innate reward mechanisms. We note, however, that optogenetic stimulation produces artificial neural activation patterns that do not fully mimic natural dopamine neuron activity.

To assess cue-evoked neural dynamics, we monitored dopamine neuron population fluorescence during optogenetic Pavlovian conditioning (Fig. 2c). As with the ChR2 experiments (Fig. 1), cues paired with ChrimsonR-mediated optogenetic activation of dopamine neurons came to reliably evoke conditioned behavior (Fig. 2d) relative to unpaired controls. In these cue-laser paired rats, we observed an increase in fluorescence at cue onset (preceding laser onset) that grew in magnitude across training (Fig. 2e,f), whereas no such cue-evoked signals emerged for unpaired control rats (Fig. 2e,f). A further trial-by-trial analysis revealed that, across training, on trials in which a CR occurred, cue-evoked dopamine neuron activity became predictive of the latency of locomotion onset: larger magnitude cue-evoked fluorescence was associated with faster conditioned response initiation (Fig. 2g,h). These results indicate that dopamine neurons develop phasic activity to CSs that they have directly established via their associated activation, in the absence of the constellation of sensory inputs that typically accompany seeking and consumption of natural rewards. Furthermore, the magnitude of phasic cue-evoked population-level dopamine neuronal activity encodes the vigor of conditioned behavior.

Cue-evoked dopamine neuron activity reflects expectation of dopamine neuron activity. On the first and last day of optogenetic conditioning, we included probe trials (25% of the total; Fig. 3a) in which cues were delivered, but the laser stimulation was omitted.

On these trials, dopamine neuron activity in paired rats decreased at the time at which laser stimulation would have been delivered (Fig. 3b). This omission-related decrease in fluorescence developed across conditioning and was not seen in unpaired controls (Fig. 3b–e). These results parallel earlier results from electrophysiological recordings of dopamine neurons demonstrating a pause in their firing during the omission of expected food or water[16], which is thought to be mediated by the recruitment of local GABAergic neuron activity[18]. Our data suggest that natural reward exposure is not necessary to engage such midbrain plasticity mechanisms in Pavlovian learning[19].

We next conducted an extinction session, during which these rats received 25 cue presentations, but no laser stimulation was delivered (Fig. 3f). This resulted in a rapid reduction, to levels observed in session 1, of the cue-evoked fluorescence spike (Fig. 3g,h), as well as the omission-related dip in fluorescence (Fig. 3i). Extinction of the neural signal tracked behavioral extinction, such that after one extinction session, behavior evoked by the cue diminished to a level comparable to that of the first training session (Fig. 3j). Thus, rapid adjustments in the population-level activity of dopamine neurons track extinction of stimulation-evoked learning. Taken together, our findings demonstrate neural encoding of the predictive relationship between these cues and direct dopamine neuron activation.

VTA and SNc dopamine neurons confer distinct motivational properties to cues. Reward-associated CSs direct actions not only by serving as reward predictors that come to evoke neural activity, but also by acquiring reward-like incentive value. Incentive value here is defined as that property of cues that lends them motivational power to attract attention and become desirable in the absence of reward, an important process that may contribute to compulsive seeking in addiction[1]. The acquisition of incentive value does not necessarily accompany the acquisition of predictive value[15], and so we next asked whether VTA and SNc dopamine-associated CSs acquired incentive value. To do this, we examined the detailed structure of behavior during Pavlovian conditioning in ChR2-conditioned groups. In response to cue presentations, Cre+ paired VTA rats (Fig. 4a) showed cue-directed approach behavior, moving to come into proximity (<1 inches) with the cue light while it was illuminated (Fig. 4b,c, Supplementary Fig. 6, and Supplementary Video 1). This 'attraction' conditioned response is a standard behavioral index of the attribution of incentive motivational value to a CS[15,20]. Notably, Cre+ paired SNc rats did not develop approach behavior (Fig. 4d–f). VTA approach probability did not relate to subjects' proximity to the cue before cue onset (Supplementary Fig. 7) and was not observed in unpaired or Cre− controls (Fig. 4b,c and Supplementary Videos 2–5). These results suggest that VTA, but not SNc, dopamine neurons confer incentive value to CSs, and this process does not require typical reward-elicited neuronal processes other than dopamine neuron activation.

Although SNc dopamine paired rats did not develop approach behavior, we observed vigorous locomotion in these rats during cue presentation that was not directed at the cue. To quantify this conditioned movement, and to compare it with the other groups, we analyzed behavioral videos using motion-tracking software to interpolate rats' positions in the experimental chamber in the periods before, during, and after cue presentations on the final day of conditioning (Fig. 5a). We used this position information to determine the frame-by-frame velocity and the distance of the rats' heads from the cue. This tracking revealed that, at cue onset, Cre+ paired SNc rats initiated rapid movement, reaching peak velocity in ~1 s (Fig. 5b). The timing of movement onset and mean velocity in the first 2 s of the cue was significantly greater for SNc rats than for Cre+ VTA paired rats. In this analysis, unpaired and Cre− controls did not show cue- or laser-evoked movement (Fig. 5a–d), consistent with our ear-
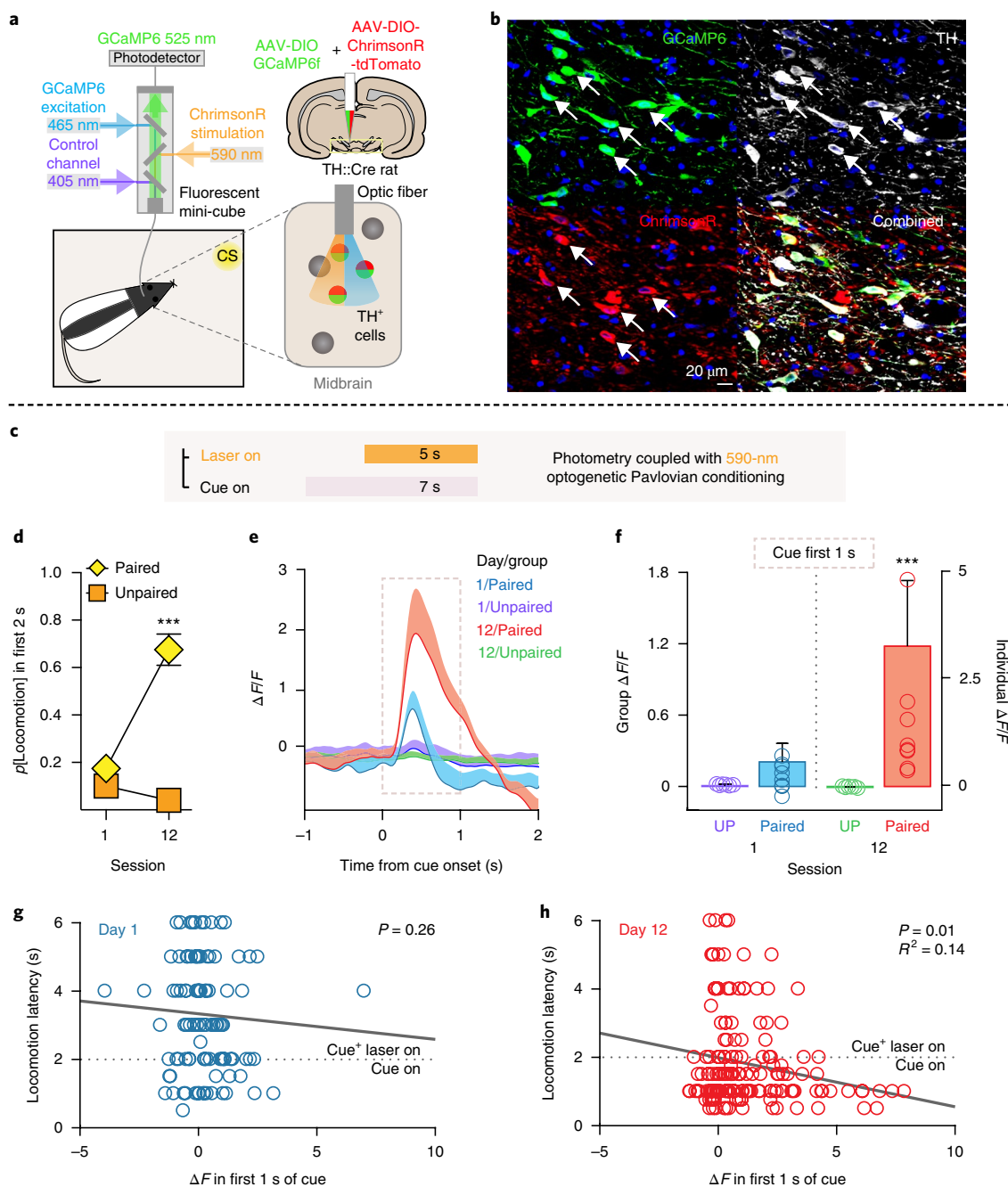
Fig. 2 | Dopamine neurons develop phasic activity in response to cues that predict their activation. a, Schematic of fiber photometry system. Fiber photometry fluorescence measurements and optogenetic stimulation in the same dopamine neurons was achieved by co-transfecting TH^{+} neurons with DIO-GCaMP6f and DIO-ChrimsonR containing AAVs. **b**, ChrimsonR and GCaMP6f coexpression in the same TH^{+} neurons in midbrain ($n = 13$). **c**, Fiber photometry measurements were made during optogenetic Pavlovian conditioning where neutral cues were paired with orange laser for activation of dopamine neurons. **d**, Cues paired with optogenetic activation of dopamine neurons with ChrimsonR ($n = 8$) developed CS properties to evoke locomotion, relative to unpaired (UP, $n = 5$) controls (two-way RM ANOVA session by group interaction, $F_{(1,12)} = 52.53$, $P < .0001$; post hoc comparison between groups). **e**, Phasic activity in dopamine neurons in response to dopamine neuron activation-paired cues developed across Pavlovian training, shown as $\Delta F/F$ of the normalized photometry signal. Shaded area represents analysis window. **f**, Summary of mean normalized $\Delta F/F$ response during the first 1 s of cue presentations on the first and last session (two-way RM ANOVA session by group interaction, $F_{(1,668)} = 48.30$, $P < 0.0001$). **g**, Scatterplot of the relationship between conditioned response latency on individual trials and change in fluorescence measured in the first 1 s after cue presentation, compared to the 1-s period before cue onset. **h**, A significant negative relationship emerged later in training, when larger changes in fluorescence during the first 1-s of the cue occurred on trials in which rats initiated conditioned locomotion faster ($n = R^2 = 0.14$, $P = 0.012$). Data are expressed as mean ± s.e.m. ***$P < 0.0001$.

lier results. During the last 5 s of cue presentations, corresponding to the laser stimulation period, SNc and VTA paired rats exhibited stable and similar movement speeds, and velocity quickly returned to low levels after cue offset (Fig. 5a–d). Together with our photome-

try data, the movement analysis suggests that Pavlovian conditioned dopamine neuron signals, in addition to spontaneous dopamine neuron signals[10,11], are involved in the generation of vigorous movements, to a greater degree in SNc than VTA dopamine neurons.
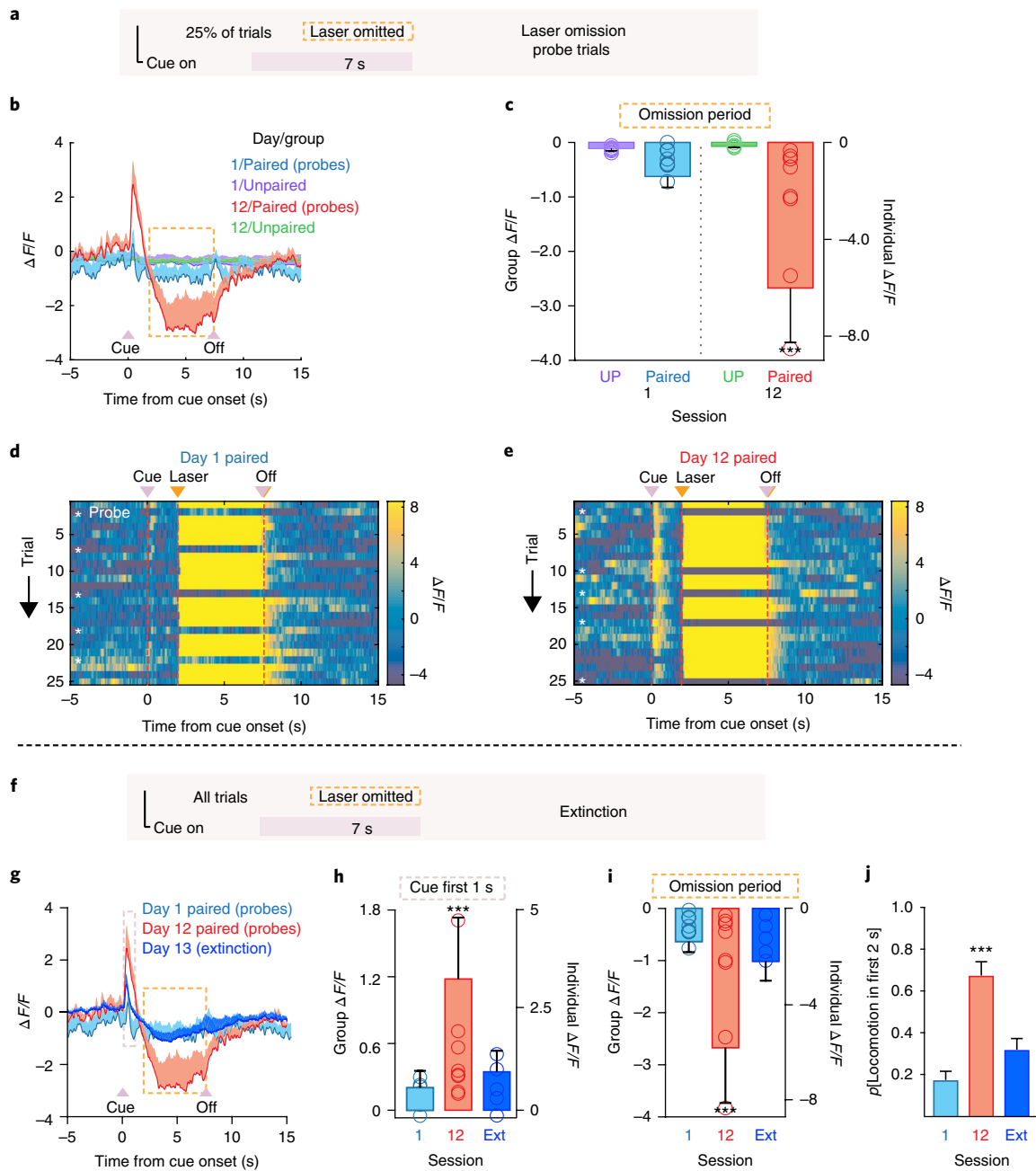
Fig. 3 | Rapid emergence and extinction of dopamine expectation signals in dopamine neurons. a, On 25% of trials in the first and last training session, laser was omitted from the paired groups. **b**, Photometry signal from probe trials in the paired groups, with unpaired control shown for comparison. On session 12 for the paired group, following the cue-evoked spike in activity, a corresponding dip in fluorescence occurs at the time when laser stimulation would have been delivered. **c**, Summary of mean normalized $\Delta F/F$ response during the omission period (session by group interaction, $F_{(1,108)} = 11.943$, $P = 0.0008$). **d,e**, Trial-by-trial heat maps for a paired rat during day 1 (**d**) and 12 (**e**) of conditioning. Cue, laser, and laser-omission related responses were evident on day 12. **f**, An extinction session occurred after training, where all cues were presented without laser stimulation. **g**, The cue- and omission-related fluorescence changes extinguishes rapidly compared with the final day of paired conditioning. **h**, Summary of mean normalized $\Delta F/F$ response during the first 1 s of cue presentations during extinction and the probe trials in session 1 and 12 (effect of session, $F_{(2,459)} = 10.03$, $P = 0.0016$). Ext, extinction. **i**, Summary of mean normalized $\Delta F/F$ during the laser omission period across sessions (effect of session, $F_{(2,179)} = 46.276$, $P < 0.0001$). **j**, Behavior evoked by the cue rapidly extinguished, compared to the final session of training (effect of session, $F_{(2,18)} = 23.37$, $P < 0.0001$). Data are expressed as mean ± s.e.m. ***$P < 0.0001$.

During extended conditioned movements, rats turned in circles in the chamber, directed contralateral to the simulation hemisphere. We quantified this movement as 'rotations' and compared their occurrence to cue-directed movement (Fig. 5e and Supplementary Fig. 8). Consistent with the experimenter-scored behavioral data (Fig. 4), motion tracking analysis revealed a cue-directed move-

ment bias for VTA paired rats, who, on average, came closer to the cue during its presentation than SNc and control rats (Fig. 5f and Supplementary Fig. 8). SNc paired rats, in contrast, showed a bias toward rotational movement, reaching a faster angular velocity than VTA rats (Fig. 5g). Although SNc rats showed an exclusive rotational movement phenotype throughout training (Fig. 5h,j),
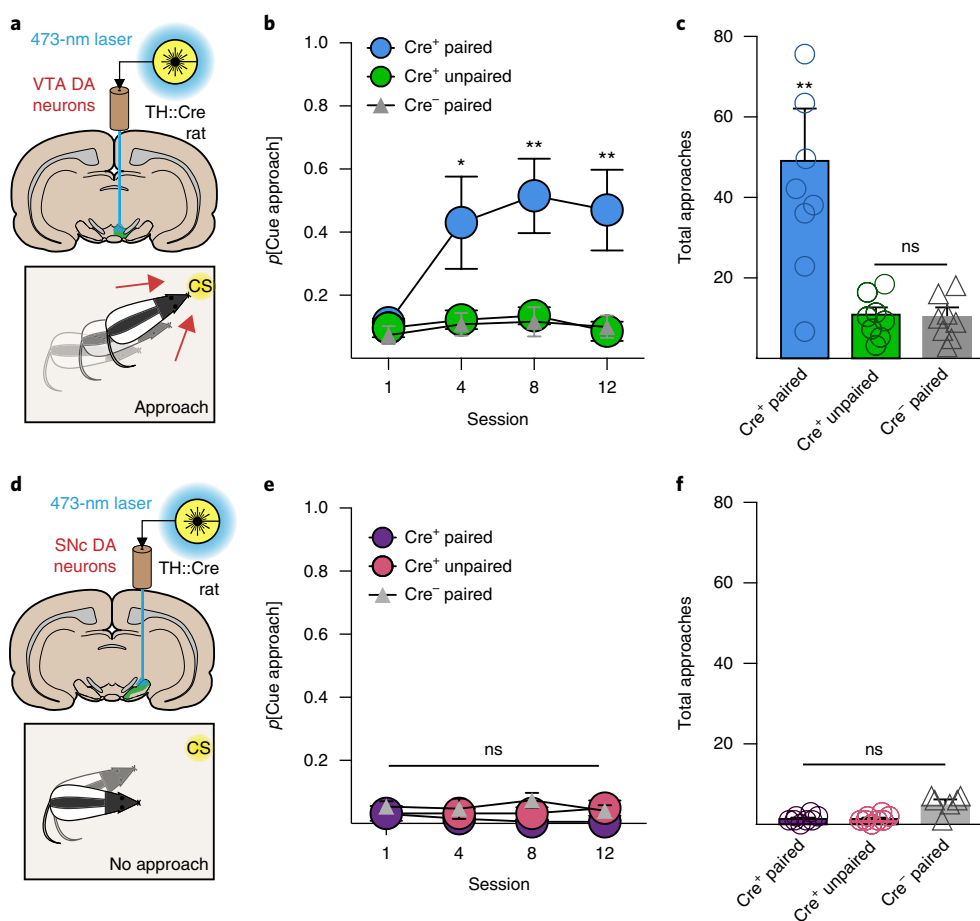
Fig. 4 | VTA, but not SNc, dopamine neurons instantiate Pavlovian cue attraction. a, VTA dopamine-paired cues support cue approach and interaction.
b, Approach and interaction with the visual cue associated with optogenetic stimulation developed for VTA Cre+ paired rats, but not control groups
(session × group interaction, $F_{(6,57)} = 2.304$, $P < 0.05$; post hoc comparisons with unpaired and Cre− groups). **c**, VTA Cre+ paired rats made significantly
more total cue approaches across training compared with controls (main effect of group, $F_{(6,57)} = 8.394$, $P < 0.001$; post hoc comparisons with unpaired and
Cre− groups). **d**, SNc dopamine-paired cues do not support approach. **e**, In contrast with the VTA group, cue approach did not develop for Cre+ paired SNc
rats relative to controls (no session × group interaction, $F_{(6,48)} = 0.637$, $P = 0.7$). **f**, SNc groups made almost zero total approaches across training. Data are
expressed as mean ± s.e.m. **$P < 0.01$.

VTA paired rats also developed rotational movement as training
progressed, resulting in a mixed cue-directed versus rotational
movement profile (Fig. 5i,j). The transition of VTA rats from purely
linear, cue-directed movement to rotational movement could reflect
the progressive recruitment of ascending serial midbrain-striatal
circuits across extended training[21], culminating in cue-related dor-
sal striatal dopamine release and behavioral control[22,23], especially if
more lateral VTA dopamine neurons, which may contribute more
directly to movement[10], are engaged. Taken together, these results
indicate that VTA and SNc dopamine neurons contribute to con-
ditioned cue attraction and conditioned movement invigoration in
distinct ways and on different timescales throughout the progres-
sion of Pavlovian learning.

In addition to being attractive, cues with incentive value can also
become desirable, in that they reinforce actions that lead to their
procurement. This process is critical for durable reward-seeking
behaviors when reward is not immediately available. Building on
our findings (Fig. 4), we next asked whether VTA and SNc dopamine
optogenetically conditioned CSs could subsequently serve as condi-
tioned or 'secondary' reinforcers to support the performance of a new
action in the absence of optogenetic stimulation (Fig. 6a). Previously
conditioned Cre+ paired VTA (Fig. 6c), but not SNc (Fig. 6d),
rats readily pressed a lever to receive conditioned cue presentations
in the absence of laser activation, indicating that the instantiation of

conditioned reinforcement, a canonical test of incentive value prop-
erties of cues, is specific to VTA dopamine neurons. Furthermore,
this indicates that, although SNc-paired cues can generate vigorous
movement (Fig. 5), the content of the signal conditioned through
SNc dopamine neurons in Pavlovian learning is fundamentally dis-
tinct from that of VTA dopamine neurons.

Finally, we assessed the primary reinforcing value of dopamine
neuron activation using an intracranial self-stimulation proce-
dure[9], in which nose pokes resulted in a brief laser train delivery,
with no associated cues (Fig. 6b). Unlike the anatomical dissocia-
tion in conditioned reinforcement, VTA and SNc dopamine neu-
ron stimulation produced similar levels of primary reinforcement
(Fig. 6e). Taken together, our results indicate that brief, phasic activ-
ity of VTA dopamine neurons is sufficient to apply incentive value
to previously neutral environmental cues to promote attraction
and create conditioned reinforcement. Alternatively, SNc dopa-
mine neuron activity imbues cues with CS properties that promote
movement invigoration more generally. Direct reinforcement of an
instrumental action, in contrast with these divergent Pavlovian cue
conditioning functions, is perhaps a common currency across VTA
and SNc dopamine neurons[9,24].

**Different striatal dopamine projections make unique contribu-
tions to Pavlovian learning.** Dopamine signaling in distinct striatal
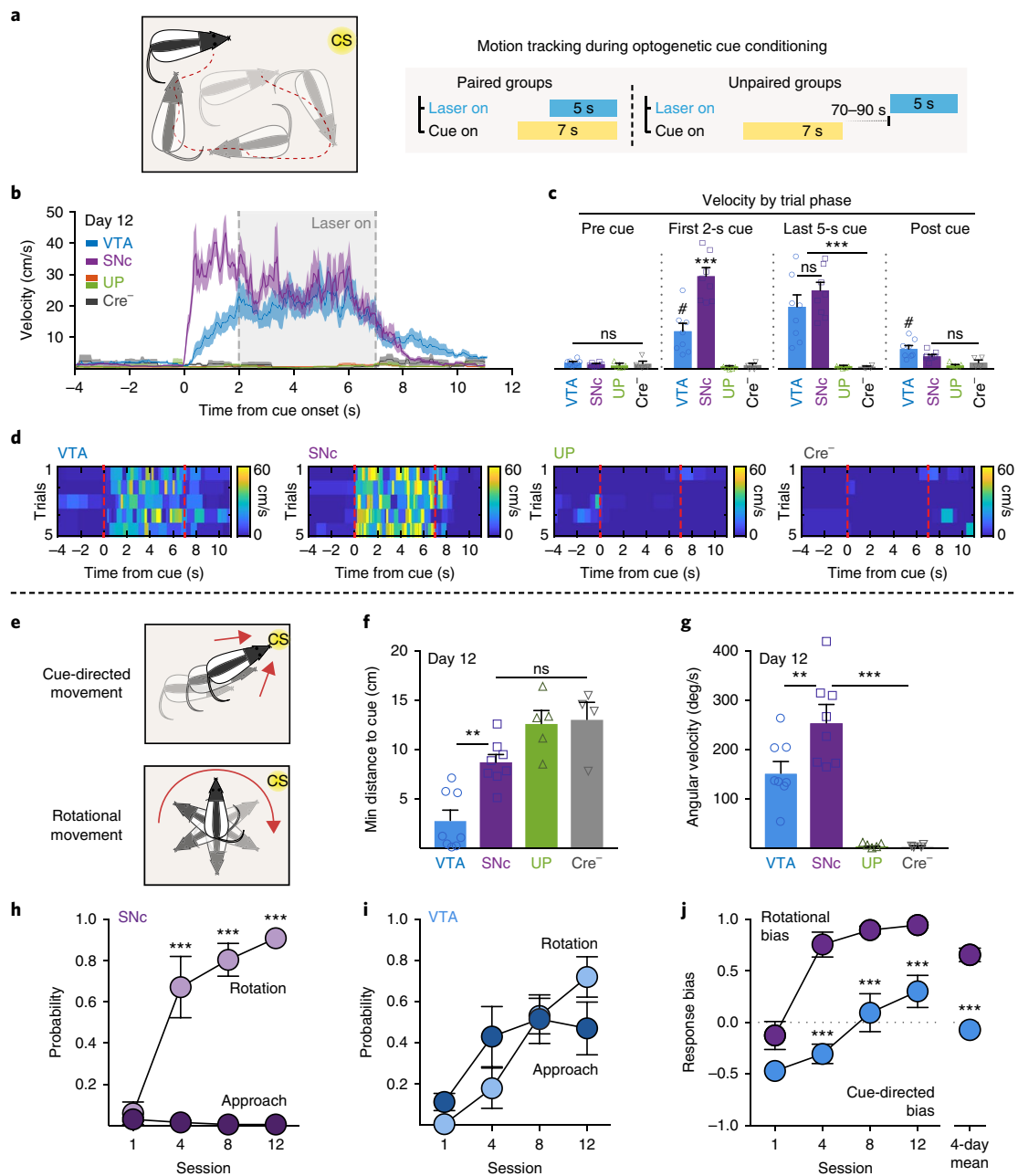
Fig. 5 | SNc dopamine neuron-paired cues evoke vigorous conditioned movement. a, Rat position before, during, and after cue presentations was quantified with automated motion tracking software. **b**, This resulted in velocity (cm/s) traces and position information for each experimental animal. **c**, Before cue onset, all rats were at rest, exhibiting low levels of movement (pre-cue velocity, no effect of group, $F_{(3,21)} = 1.165$, $P = 0.347$). Cue onset elicited rapid, vigorous movement for SNc cue paired rats ($n = 8$), relative to VTA paired ($n = 8$) and unpaired (UP, $n = 13$) and Cre⁻ ($n = 11$) controls (first 2-s velocity, effect of group, $F_{(3,21)} = 32.39$, $P < 0.0001$; ***post hoc comparison versus VTA and UP, $P < 0.0001$; #post hoc comparison versus UP, $P = 0.01$). SNc and VTA paired rats exhibited similar sustained velocity during the rest of the cue and laser period, whereas UP and Cre⁻ controls remained immobile (last 5-s cue, effect of group, $F_{(3,21)} = 16.45$, $P < 0.0001$; post hoc comparison to UP). **d**, Heat maps depicting velocity on individual trials for a representative rat from each group. UP and Cre⁻ rats exhibited almost no movement. **e**, Cue-directed movement (approach) and rotational movement on the final session were compared using the automated behavior tracking data. **f**, VTA-paired rats were biased toward cue-directed movement, reaching a significantly smaller minimum distance to the cue, as compared with SNc and control groups, who did not differ (effect of group, $F_{(3,21)} = 18.06$, $P < 0.0001$, post hoc comparison between groups). **g**, SNc paired rats showed a bias toward rotational movement, reaching a faster angular velocity than VTA rats (effect of group, $F_{(3,21)} = 17.02$, $P < 0.0001$, post hoc comparison between groups). **h**, Directly comparing the likelihood of each type of movement, only cue-evoked rotational movement developed for SNc Cre⁺ paired rats, which was expressed exclusively on nearly every trial by the end of training (interaction of CR type × session, $F_{(3,21)} = 30.88$, $P < 0.0001$; post hoc comparison between CR types). **i**, VTA paired rats showed cue-directed and rotational movement, which became intermixed across Pavlovian training (interaction of CR type × session, $F_{(3,21)} = 4.341$, $P = 0.016$). **j**, To quantify rats' cue-directed/rotational bias, we calculated a CR score, consisting of $(X + Y)/2$, where response bias, X, equals (number of turns – number of approaches)/(number of turns + number of approaches), and probability difference, Y, equals (p[rotation] – p[approach]). VTA rats transitioned from an initial cue-directed bias to a mixed cue-directed/rotational score, whereas SNc rats showed an early and stable rotational bias (interaction of group × session, $F_{(3,42)} = 3.933$, $P = 0.015$); post hoc comparison between groups; unpaired two-tailed t test on 4-d mean, $t_{14} = 7.287$, $P < 0.0001$. Data are expressed as mean ± s.e.m. ***$P < 0.0001$.
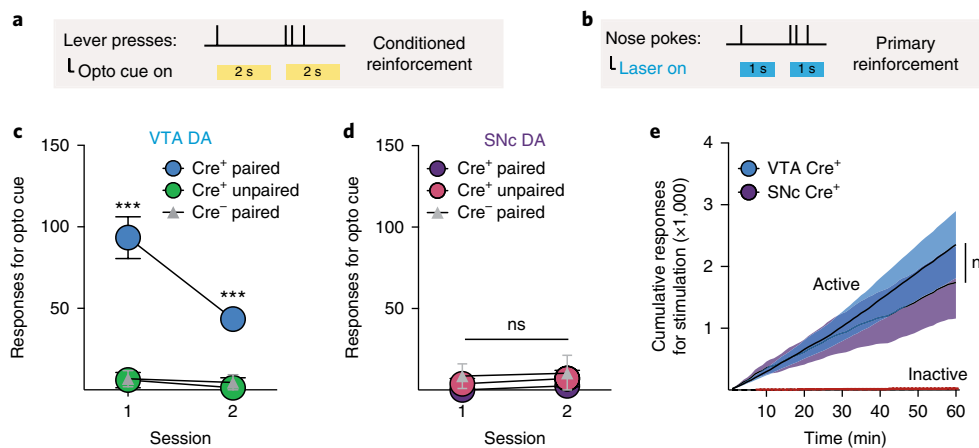
Fig. 6 | VTA and SNc dopamine neurons differentially create conditioned, but not primary, reinforcement. a, Conditioned reinforcement test, in which lever presses produced the cue previously paired with dopamine neuron stimulation, but no laser. **b**, Primary reinforcement test, in which nose poke responses produced optogenetic stimulation of dopamine neurons. **c**, VTA Cre+ paired rats made instrumental responses for cue presentations in the absence of laser, relative to controls (two-way RM ANOVA, main effect of group, $F_{(2,19)} = 27.18$, $P < 0.0001$; post hoc comparisons with unpaired and Cre− groups). **d**, SNc Cre+ paired rats did not respond for cue presentations, relative to controls (two-way RM ANOVA, no effect of group, $F_{(2,16)} = 1.407$, $P = 0.274$). **e**, VTA ($n = 16$) and SNc ($n = 13$) Cre+ rats made a similar number of instrumental responses for dopamine neuron activation (two-way RM ANOVA, no effect of group, $F_{(1,27)} = 0.227$, $P = 0.638$). Data are expressed as mean ± s.e.m. ***$P < 0.0001$.

compartments can modulate the value of reward-associated cues[25–28], but it is unknown whether phasic activity from distinct dopamine projections to different striatal areas can support Pavlovian learning. Given this mesostriatal complexity, and that the VTA manipulations described above could affect dopamine projections to non-striatal targets[29], we next determined whether dopamine neurons projecting into subregions of the striatum would assign CS and incentive properties to optogenetically conditioned cues. We transfected the striatum of TH-Cre+ rats with a retrogradely transported AAV vector containing ChR2, which produced robust expression in dopamine neurons in the midbrain (Fig. 7a,b). Ex vivo electrophysiological recordings revealed that ChR2-expressing dopamine neurons projecting to the ventral striatum/nucleus accumbens (NAc) and dorsal striatum (DS) reliably fired action potentials following 20-Hz blue light stimulation (Fig. 7c–e and Supplementary Fig. 9). In separate groups of rats, we targeted injections to dopamine terminals in the NAc core, NAc medial shell, or DS, which resulted in projection-defined expression patterns among TH+ neurons in the midbrain (Supplementary Fig. 10). Cell bodies of dopamine projections to the shell were concentrated in the ventromedial VTA (Fig. 7g and Supplementary Fig. 10), projections to the core were concentrated in the dorsolateral VTA (Fig. 7h and Supplementary Fig. 10), and DS projections occupied the medial-lateral extent of the SNc (Fig. 7i and Supplementary Fig. 10). We targeted optic fibers over the midbrain in these animals for projection-specific activation during optogenetic conditioning (Fig. 7f–i). Cues paired with VTA-Core[DA] and SNc-DS[DA], but not VTA-Shell[DA], projectors evoked conditioned behavior relative to unpaired controls (Fig. 7j). Examining the detail of the behavioral responses in our projection-specific experiments, we found that only VTA-Core[DA] neurons supported cue approach (Fig. 7k,l), although SNc-DS[DA] neurons preferentially promoted rotational movement during cue presentations (Fig. 7m,n).

Finally, after dopamine projection-specific optogenetic conditioning (Fig. 8a), only VTA-Core[DA]-associated cues acted as conditioned reinforcers (Fig. 8b,d). In contrast, primary reinforcement was similar for all of the projection groups (Fig. 8c,e). Thus, dopamine neurons confer heterogeneous conditioned motivational signals about cues in a projection-defined manner, with the projection to the NAc core mediating the acquisition of incentive value.

Discussion

We trained rats to associate sensory cues with optogenetic activation of dopamine neurons. We found that, by virtue of a temporal pairing, the cues acquired CS properties that allowed them to evoke conditioned behaviors and conditioned dopamine neuron activity. Notably, the topography of behavior evoked by conditioned cues varied according to which dopamine neuron subpopulation was targeted. These results demonstrate a fundamental dissociation in the function of dopamine neurons in Pavlovian conditioned motivation, in which VTA-associated cues acquire incentive motivational value, and SNC-associated cues invigorate intense locomotion. Furthermore, we found that the incentive value function was specific to NAc core-projecting, but not NAc shell-projecting, dopamine neurons. Taken together, our results reveal highly specialized functional isolation for mesostriatal dopamine circuits in distinct components of Pavlovian reward.

Dopamine neurons have heterogeneous motivational functions. Our results confirm a longstanding, fundamental assumption in reward neuroscience: that activity in dopamine neurons can create Pavlovian conditioned stimuli that elicit conditioned behaviors. Although our activation can be seen as essentially mimicking the phasic activity proposed to act as a reward prediction error, we found that dopamine neurons did not merely update Pavlovian associations between cues and external rewards[4], but rather directly conferred value and were able to do so in the absence of normal reward-activated sensory inputs and the other corresponding brain processes that typically accompany natural reward exposure and consumption. Our findings extend those of previous studies[7] by showing that discrete, transient cues become CSs via association with relatively brief bursts (~1–5 s) of dopamine neuron activity. Notably, our results define the default behavioral responses conditioned by cue-paired phasic dopamine signals in relation to different dopamine neuron populations.

We found that CS instantiation is a function that is generally present in the major dopamine neuron output systems in the ventral midbrain, the VTA and SNc (Fig. 1). We found that these conditioned stimuli came to evoke population-level activity in dopamine neurons themselves (Fig. 2), consistent with what has been previously demonstrated with single-unit recordings during natural (e.g., food) cue conditioning[13,16,30]. This cue-evoked dopamine neuron
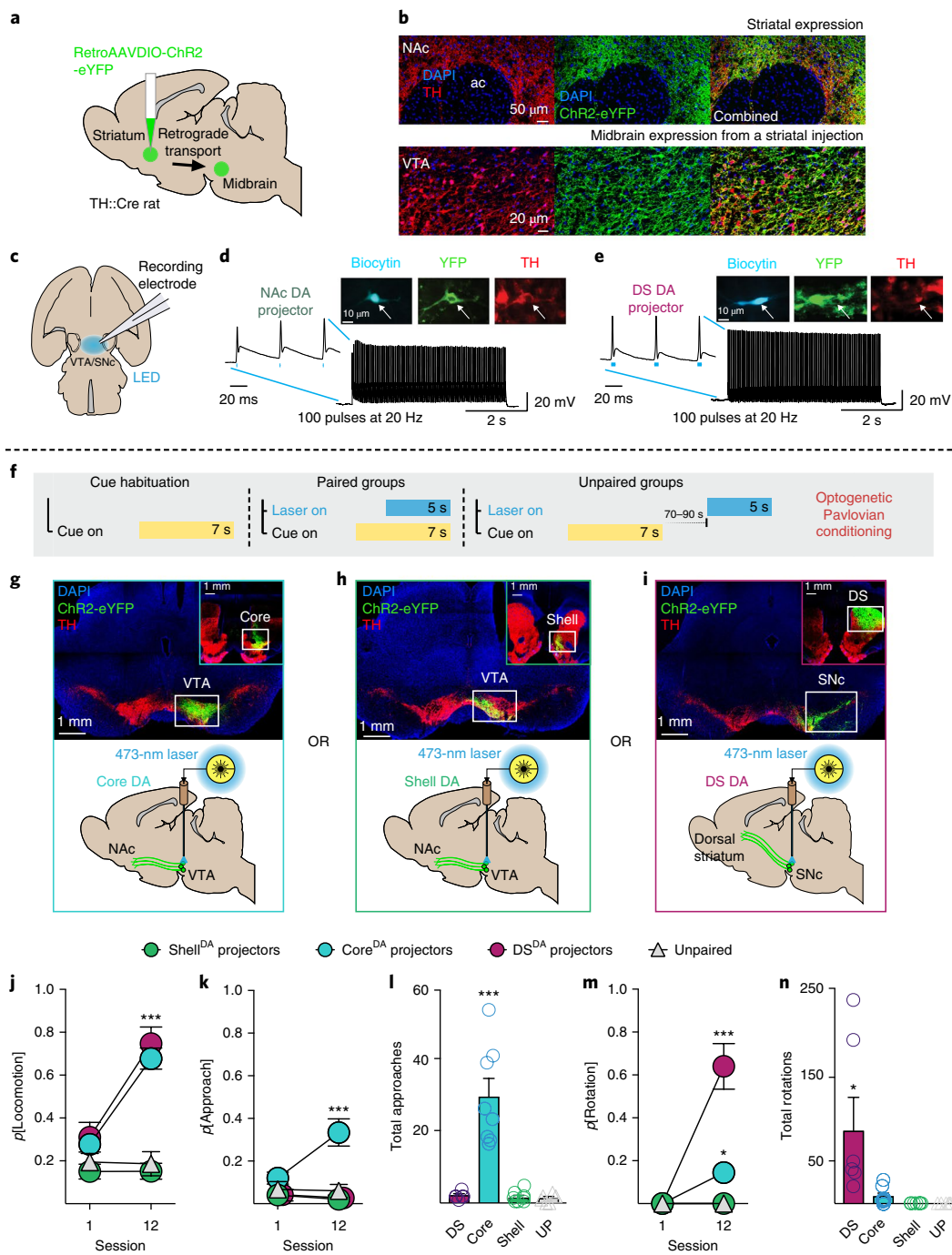
Fig. 7 | Striatal projection-specific instantiation of Pavlovian CS properties. a, Viral strategy for targeting specific dopamine projections via retrograde AAV-DIO-ChR2 transport. **b**, Transfection in striatum of TH-Cre rats led to robust expression of ChR2-eYFP in TH⁺ cells in the midbrain. **c**, Retrogradely targeted neurons in the VTA and SNc were recorded in an ex vivo preparation. **d**, Example ChR2 retrogradely transfected nucleus accumbens-projecting dopamine neuron with high fidelity spike trains in response to a 5-s, 100-pulse, 20-Hz stimulation. **e**, Example retrogradely-transfected DS-projecting dopamine neuron with high fidelity spike trains in response to blue LED pulses. **f**, Rats underwent optogenetic Pavlovian cue conditioning of different dopamine neuron projections. **g**, Retrograde AAV injections targeted to the NAc core resulted in expression in VTA, where optic fibers were placed. **h**, Injections targeted to the NAc shell resulted in expression in the VTA. **i**, Injections targeted to the DS resulted in expression in the SNc. **j**, SNc-DS^{DA} ($n = 6$) and VTA-Core^{DA} ($n = 8$), but not VTA-Shell^{DA} ($n = 8$) paired rats developed conditioned behavior (that is, locomotion) in response to laser-paired cues, relative to unpaired rats (two-way RM ANOVA, main effect of group $F_{(3,24)} = 28.17$, $P < 0.0001$; group by session interaction, $F_{(3,24)} = 13.88$, $P < 0.0001$; post hoc comparison relative to the unpaired group). **k**, Only VTA-Core^{DA} paired rats developed conditioned approach to the cue (main effect of group $F_{(3,24)} = 19.54$, $P < 0.0001$; group by session interaction, $F_{(3,24)} = 5.127$, $P = 0.007$; post hoc comparison relative to the unpaired group). **l**, Only VTA-Core^{DA} rats made a significant number of approaches across training (main effect of group, $F_{(3,24)} = 24.55$, $P < 0.0001$, post hoc comparison to unpaired (UP) group). **m**, SNc-DS^{DA} rats preferentially developed conditioned rotation, reflecting vigorous movement, in response to the Pavlovian cue (main effect of group $F_{(3,24)} = 33.09$, $P < 0.0001$; group by session interaction, $F_{(3,24)} = 33.09$, $P < 0.0001$; post hoc comparison relative to the unpaired group). **n**, Only SNc-DS^{DA} rats made a significant number of rotations across training, relative to unpaired controls (main effect of group $F_{(3,24)} = 5.486$, $P = 0.005$, post hoc comparison relative to the unpaired group). Data are expressed as mean ± s.e.m. ***$P < 0.0001$.

activity evinced a relationship with behavior as a consequence of Pavlovian conditioning, and fluctuations in this signal tracked a learned expectation of dopamine neuron activity (Fig. 3). Thus, a basic function of dopamine neurons in Pavlovian conditioning is to accumulate and signal predictive information about the probability of future dopamine neuron activity, a phenomenon that fundamentally does not require elaboration of further brain processes normally triggered by an external food reward beyond the elicitation of dopamine activity itself. Once learned, the phasic, cue-evoked dopamine neuron signals functionally represent the motivational value of cues that predict future dopamine neuron activity, which manifests as the vigor or intensity of conditioned behavior[5,31,32], the details of which depend on the dopamine projection engaged. Given the absence of an external reward, our findings do not reveal how dopamine neuron activation may contribute to associations among specific sensory and/or identity properties of external rewards and the cues that predict them. Dopamine can contribute to both a general and an outcome-specific form of learning in natural reward conditioning[33,34], suggesting that the sensory qualities and concomitant brain dynamics of the unconditioned stimulus that produce dopamine neuron activation are likely to be critical for determining the content of the association learned. Our experiments probed the function of dopamine systems absent outcome-specific information, revealing fundamental roles of dopamine neurons that may well be recruited in situations requiring more complex associations.

One of our primary findings is that dopamine neurons in the VTA and SNc exhibited divergent conditioned motivational functions. VTA, but not SNc, dopamine neurons conferred a signal that made those cues attractive and reinforcing on their own (Figs. 4 and 6), two properties demonstrating the incentive value of reward cues, and most likely the explanation for the behavioral patterns that we observed. These results build on a large body of research implicating dopamine signaling in cue attraction and conditioned reinforcement[15,20,26,27,35,36] by showing that some dopamine neurons create these properties during Pavlovian conditioning in the absence of reward receipt or consumption. We found that SNc dopamine neurons, alternatively, conferred a more general movement invigoration signal (Fig. 5); cues paired with their activation evoked vigorous movement not directed at the cue, and they failed to serve as conditioned reinforcers. Thus, distinct components of conditioned reward are represented and controlled by different dopamine output systems. Although nigrostriatal dopamine neurons do not appear to instantiate incentive value per se in Pavlovian conditioned stimuli, they do however confer their own important motivational properties, evidenced here by vigorous cue-evoked movement, perhaps akin to a learned 'motor motivation'[37]. In the absence of a VTA-mediated incentive component to orient and guide animals to a specific target, direct engagement of SNc-dopamine-mediated learning might manifest as a general increase in locomotion. Notably, dorsal striatal dopamine transmission is not required for the expression of approach to Pavlovian conditioned cues[38], but the dorsal striatum is necessary for the ability of Pavlovian conditioned cues to invigorate ongoing instrumental actions[39], which could be an expression of the conditioned movement invigoration that we observed. Thus, in natural learning situations involving external rewards, motivation to engage in specific movements and actions, signaled by SNc dopamine, would be incorporated with motivation to achieve specific rewarding outcomes, signaled via VTA dopamine. Future work will be needed to explore the motivational content conferred by SNc dopamine neurons, how dorsomedial and dorsolateral projecting dopamine neurons may differ[40–42], and how VTA and SNc dopamine circuits interact across learning to fine-tune reward seeking.

We found that at least some types of movements reflect a conditioned state resulting from an association between dopamine neuron activity and the presentation of external sensory cues: uncued dopamine neuron activation did not generate locomotion.
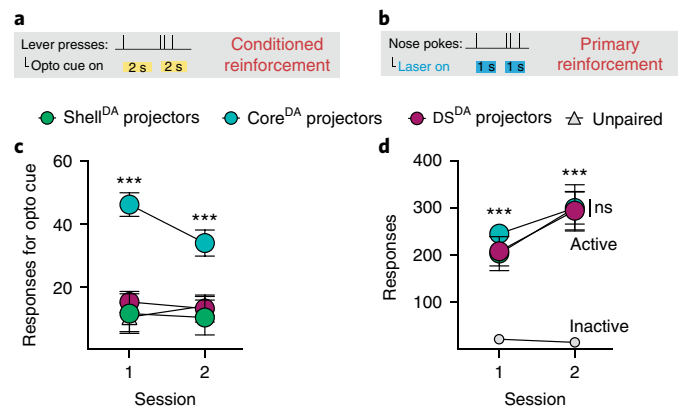
Fig. 8 | Striatal projection-specific control of conditioned, but not primary, reinforcement. a, Optic fibers were implanted over the VTA or SNc for selective optogenetic stimulation of NAc core-projecting, NAc shell-projecting, or DS-projecting dopamine neurons. **b,d**, In a test of conditioned reinforcement for an optogenetically conditioned Pavlovian cue, VTA-Core[DA] Cre+ paired rats ($n = 9$) responded robustly for cue presentations, relative to VTA-Shell[DA] Cre+ paired ($n = 7$) and SNc-DS[DA] Cre+ paired rats ($n = 9$), whereas VTA-Shell[DA] paired and SNc-DS[DA] paired rats were no different from unpaired ($n = 9$) controls (two-way repeated measures ANOVA, main effect of group, $F_{(3,30)} = 13.08$, $P < 0.0001$; post hoc comparisons between groups). **c,e**, In a test of primary reinforcement, VTA-Core[DA] ($n = 6$), VTA-Shell[DA] ($n = 6$), and SNc-DS[DA] ($n = 8$) groups made a similar number of responses for optogenetic stimulation (two-way RM ANOVA, no effect of group, $F_{(2,16)} = 0.142$, $P = 0.869$; post hoc comparison relative to inactive responses). Data are expressed as mean ± s.e.m. ***$P < 0.0001$.

This provides context for important recent work assessing the role of dopamine neuron activity during self-initiated or spontaneous movements[10–12]. Our findings suggest that dopamine-mediated movements that are not self-generated are gated by the presence of salient sensory stimuli. Notably, movement patterning is dependent on sensory input[43], and conditioning with visual cues can improve movement deficits in Parkinson's patients[44]. Thus, external signals are critical for normal expression of movement, and our results suggest that dopamine neurons contribute to this process perhaps by assigning motivational value to cues, allowing them to draw attention and invigorate actions, shaping locomotion.

Dopamine circuit-specific functions in Pavlovian reward learning. Our results are among the first to isolate distinct conditioned motivational functions for phasic activity among specific dopamine projections (Figs. 7 and 8), providing an important step toward understanding how dopamine neurons orchestrate Pavlovian reward moment by moment at the circuit level. We found that NAc core and dorsal striatal projecting dopamine neurons created conditioned stimuli out of previously neutral sensory cues and assigned motivational value to promote cue attraction and conditioned reinforcement[15,25,28], and movement invigoration, respectively. NAc medial shell dopamine neurons, however, did not confer CS properties, even though their optogenetic activation produced primary reinforcement comparable to that of the other dopamine projections. Many previous studies have implicated NAc shell dopamine signaling in reward learning and incentive motivation[27,45], but our results suggest that, although medial shell dopamine release may be engaged during reward learning, phasic activity in shell-projecting dopamine neurons is not sufficient to drive cue learning per se. It is possible that medial shell dopamine actions in Pavlovian learning may functionally act on longer timescales during behavior, which are not captured in the current studies. In addition, medial shell

dopamine, and activity from shell medium spiny neurons (MSNs), may more directly control reward consumption and evaluation, rather than prediction[46–48].

Among dopamine neurons, there is considerable genetic, anatomical, and physiological diversity[8]. Although some properties of medial accumbens shell dopamine neurons have been compared to those projecting to the dorsal striatum, prefrontal cortex, and amygdala[49], less is known about how medial shell and core inputs differ. The medial shell may receive relatively more input from VTA neurons that co-release dopamine and glutamate and that are concentrated in the medial VTA[8], and medial shell neurons have unique connectivity patterns in the VTA compared with lateral accumbens neurons[50]. In the rat, medial shell MSNs project most heavily back to the VTA, while lateral shell/core MSNs project more broadly, including to the SNc. This potentially greater circuit access may be permissive for rapid dopamine signaling in the NAc core, but not shell, to engage Pavlovian learning mechanisms that produce conditioned behaviors, as in our experiments.

Conclusions

In summary, we found that brief, phasic dopamine neuron activity can create a CS in the absence of external reward. Our results provide important context to previous research, suggesting a uniform contribution of dopamine neurons to stimulus-reward learning[30] by showing that considerable heterogeneity exists in the functional content of information induced by different dopamine neurons during conditioning[41]. Circuit-defined dopamine neuron activity induced learning of cue-guided behavior by directing behavior toward cues themselves or by allowing cues to more nonspecifically invigorate movement. The combination of both forms of cue-guided behavior may be necessary for successful reward-seeking under changing conditions and environments. Finally, because the animals in our studies never received a traditional food reward, yet developed the type of cue-evoked behaviors typically seen during conditioned reward seeking, our findings suggest that dopamine systems are specialized for supporting and engendering circuit-specific adaptations that promote the expression of discrete classes of motivated behavior in response to reward cues. Although these sensory cues may normally signal opportunity for reward, actual commerce with an external reward is not required for the emergence of cue-evoked behaviors and the acquisition of conditioned incentive motivation by cues.

Methods

Methods, including statements of data availability and any associated accession codes and references, are available at https://doi.org/10.1038/s41593-018-0191-4.

References

1. Robinson, T. E. & Berridge, K. C. The neural basis of drug craving: an incentive-sensitization theory of addiction. *Brain Res. Brain Res. Rev.* **18**, 247–291 (1993).
2. Dauer, W. & Przedborski, S. Parkinson's disease: mechanisms and models. *Neuron* **39**, 889–909 (2003).
3. Keiflin, R. & Janak, P. H. Dopamine prediction errors in reward learning and addiction: from theory to neural circuitry. *Neuron* **88**, 247–263 (2015).
4. Steinberg, E. E. et al. A causal link between prediction errors, dopamine neurons and learning. *Nat. Neurosci.* **16**, 966–973 (2013).
5. Hamid, A. A. et al. Mesolimbic dopamine signals the value of work. *Nat. Neurosci.* **19**, 117–126 (2016).
6. Chang, C. Y. et al. Brief optogenetic inhibition of dopamine neurons mimics endogenous negative reward prediction errors. *Nat. Neurosci.* **19**, 111–116 (2016).
7. Tsai, H.-C. et al. Phasic firing in dopaminergic neurons is sufficient for behavioral conditioning. *Science* **324**, 1080–1084 (2009).
8. Morales, M. & Margolis, E. B. Ventral tegmental area: cellular heterogeneity, connectivity and behaviour. *Nat. Rev. Neurosci.* **18**, 73–85 (2017).
9. Witten, I. B. et al. Recombinase-driver rat lines: tools, techniques, and optogenetic application to dopamine-mediated reinforcement. *Neuron* **72**, 721–733 (2011).
10. Howe, M. W. & Dombeck, D. A. Rapid signalling in distinct dopaminergic axons during locomotion and reward. *Nature* **535**, 505–510 (2016).
11. Dodson, P. D. et al. Representation of spontaneous movement by dopaminergic neurons is cell-type selective and disrupted in parkinsonism. *Proc. Natl. Acad. Sci. USA* **113**, E2180–E2188 (2016).
12. da Silva, J. A., Tecuapetla, F., Paixão, V. & Costa, R. M. Dopamine neuron activity before action initiation gates and invigorates future movements. *Nature* **554**, 244–248 (2018).
13. Cohen, J. Y., Haesler, S., Vong, L., Lowell, B. B. & Uchida, N. Neuron-type-specific signals for reward and punishment in the ventral tegmental area. *Nature* **482**, 85–88 (2012).
14. Day, J. J., Roitman, M. F., Wightman, R. M. & Carelli, R. M. Associative learning mediates dynamic shifts in dopamine signaling in the nucleus accumbens. *Nat. Neurosci.* **10**, 1020–1028 (2007).
15. Flagel, S. B. et al. A selective role for dopamine in stimulus-reward learning. *Nature* **469**, 53–57 (2011).
16. Waelti, P., Dickinson, A. & Schultz, W. Dopamine responses comply with basic assumptions of formal learning theory. *Nature* **412**, 43–48 (2001).
17. Cui, G. et al. Concurrent activation of striatal direct and indirect pathways during action initiation. *Nature* **494**, 238–242 (2013).
18. Eshel, N. et al. Arithmetic and local circuitry underlying dopamine prediction errors. *Nature* **525**, 243–246 (2015).
19. Stuber, G. D. et al. Reward-predictive cues enhance excitatory synaptic strength onto midbrain dopamine neurons. *Science* **321**, 1690–1692 (2008).
20. Berridge, K. C. The debate over dopamine's role in reward: the case for incentive salience. *Psychopharmacol. (Berl.)* **191**, 391–431 (2007).
21. Haber, S. N., Fudge, J. L. & McFarland, N. R. Striatonigrostriatal pathways in primates form an ascending spiral from the shell to the dorsolateral striatum. *J. Neurosci.* **20**, 2369–2382 (2000).
22. Belin, D. & Everitt, B. J. Cocaine seeking habits depend upon dopamine-dependent serial connectivity linking the ventral with the dorsal striatum. *Neuron* **57**, 432–441 (2008).
23. Willuhn, I., Burgeno, L. M., Everitt, B. J. & Phillips, P. E. M. Hierarchical recruitment of phasic dopamine signaling in the striatum during the progression of cocaine use. *Proc. Natl. Acad. Sci. USA* **109**, 20703–20708 (2012).
24. Ilango, A. et al. Similar roles of substantia nigra and ventral tegmental dopamine neurons in reward and aversion. *J. Neurosci.* **34**, 817–822 (2014).
25. Saunders, B. T. & Robinson, T. E. The role of dopamine in the accumbens core in the expression of Pavlovian-conditioned responses. *Eur. J. Neurosci.* **36**, 2521–2532 (2012).
26. Taylor, J. R., & Robbins, T. W.. Enhanced behavioural control by conditioned reinforcers following microinjections of d-amphetamine into the nucleus accumbens. *Psychopharmacol. (Berl.)* **84**, 405–412 (1984).
27. Kelley, A. E. & Delfs, J. M. Dopamine and conditioned reinforcement. *Psychopharmacol. (Berl.)* **103**, 187–196 (1991).
28. Di Ciano, P., Cardinal, R. N., Cowell, R. A., Little, S. J. & Everitt, B. J. Differential involvement of NMDA, AMPA/kainate, and dopamine receptors in the nucleus accumbens core in the acquisition and performance of pavlovian approach behavior. *J. Neurosci.* **21**, 9471–9477 (2001).
29. Swanson, L. W. The projections of the ventral tegmental area and adjacent regions: a combined fluorescent retrograde tracer and immunofluorescence study in the rat. *Brain Res. Bull.* **9**, 321–353 (1982).
30. Eshel, N., Tian, J., Bukwich, M. & Uchida, N. Dopamine neurons share common response function for reward prediction error. *Nat. Neurosci.* **19**, 479–486 (2016).
31. Wassum, K. M., Ostlund, S. B., Loewinger, G. C. & Maidment, N. T. Phasic mesolimbic dopamine release tracks reward seeking during expression of Pavlovian-to-instrumental transfer. *Biol. Psychiatry* **73**, 747–755 (2013).
32. McClure, S. M., Daw, N. D. & Montague, P. R. A computational substrate for incentive salience. *Trends Neurosci.* **26**, 423–428 (2003).
33. Sharpe, M. J. et al. Dopamine transients are sufficient and necessary for acquisition of model-based associations. *Nat. Neurosci.* **20**, 735–742 (2017).
34. Dayan, P. & Berridge, K. C. Model-based and model-free Pavlovian reward learning: revaluation, revision, and revelation. *Cogn. Affect. Behav. Neurosci.* **14**, 473–492 (2014).
35. Pascoli, V., Terrier, J., Hiver, A. & Lüscher, C. Sufficiency of mesolimbic dopamine neuron stimulation for the progression to addiction. *Neuron* **88**, 1054–1066 (2015).
36. Burgess, C. P. et al. High-yield methods for accurate two-alternative visual psychophysics in head-fixed mice. *Cell Rep.* **20**, 2513–2524 (2017).
37. Mazzoni, P., Hristova, A. & Krakauer, J. W. Why don't we move faster? Parkinson's disease, movement vigor, and implicit motivation. *J. Neurosci.* **27**, 7105–7116 (2007).

38. Fraser, K. M. & Janak, P. H. Long-lasting contribution of dopamine in the nucleus accumbens core, but not dorsal lateral striatum, to sign-tracking. *Eur. J. Neurosci.* **46**, 2047–2055 (2017).

39. Corbit, L. H. & Janak, P. H. Inactivation of the lateral but not medial dorsal striatum eliminates the excitatory impact of Pavlovian stimuli on instrumental responding. *J. Neurosci.* **27**, 13977–13981 (2007).

40. Lerner, T. N. et al. Intact-brain analyses reveal distinct information carried by SNc dopamine subcircuits. *Cell* **162**, 635–647 (2015).

41. Parker, N. F. et al. Reward and choice encoding in terminals of midbrain dopamine neurons depends on striatal target. *Nat. Neurosci.* **19**, 845–854 (2016).

42. Matsumoto, M. & Hikosaka, O. Two types of dopamine neuron distinctly convey positive and negative motivational signals. *Nature* **459**, 837–841 (2009).

43. Klockgether, T., Borutta, M., Rapp, H., Spieker, S. & Dichgans, J. A defect of kinesthesia in Parkinson's disease. *Mov. Disord.* **10**, 460–465 (1995).

44. Azulay, J. P. et al. Visual control of locomotion in Parkinson's disease. *Brain* **122**, 111–120 (1999).

45. Saddoris, M. P., Cacciapaglia, F., Wightman, R. M. & Carelli, R. M. Differential dopamine release dynamics in the nucleus accumbens core and shell reveal complementary signals for error prediction and incentive motivation. *J. Neurosci.* **35**, 11572–11582 (2015).

46. Bassareo, V. & Di Chiara, G. Differential responsiveness of dopamine transmission to food-stimuli in nucleus accumbens shell/core compartments. *Neuroscience* **89**, 637–641 (1999).

47. Richard, J. M. & Berridge, K. C. Nucleus accumbens dopamine/glutamate interaction switches modes to generate desire versus dread: D(1) alone for appetitive eating but D(1) and D(2) together for fear. *J. Neurosci.* **31**, 12866–12879 (2011).

48. Millan, E. Z., Kim, H. A. & Janak, P. H. Optogenetic activation of amygdala projections to nucleus accumbens can arrest conditioned and unconditioned alcohol consummatory behavior. *Neuroscience* **360**, 106–117 (2017).

49. Margolis, E. B., Mitchell, J. M., Ishikawa, J., Hjelmstad, G. O. & Fields, H. L. Midbrain dopamine neurons: projection target determines action potential duration and dopamine D(2) receptor inhibition. *J. Neurosci.* **28**, 8908–8913 (2008).

50. Yang, H. et al. Nucleus accumbens subnuclei regulate motivated behavior via direct inhibition and disinhibition of VTA dopamine subpopulations. *Neuron* **97**, 434–449.e4 (2018).

Acknowledgements

Author contributions

B.T.S. and P.H.J. designed the experiments. B.T.S. collected and analyzed data from ChR2 experiments. B.T.S. and J.M.R. collected and analyzed the photometry data. E.B.M. collected and analyzed the ex vivo physiology data. B.T.S. and P.H.J. wrote the manuscript with input from all the authors.

Competing interests

The authors declare no competing interests.

Additional information

Supplementary information is available for this paper at https://doi.org/10.1038/s41593-018-0191-4.

Reprints and permissions information is available at www.nature.com/reprints.

Correspondence and requests for materials should be addressed to B.T.S. or P.H.J.

Publisher's note: Springer Nature remains neutral with regard to jurisdictional claims in published maps and institutional affiliations.

Methods

Subjects. Male and female TH-Cre transgenic rats (on a Long-Evans background) were used in these studies. These rats express Cre recombinase under the control of the tyrosine hydroxylase (TH) promoter in over 60% of all TH+ neurons in the midbrain[9]. Wild-type littermates (TH-Cre−) were used as controls. After surgery rats were individually housed with ad libitum access to food and water on a 0700 to 1900 light/dark cycle (lights on at 0700). All rats weighed >250 g at the time of surgery and were 5–9 months old at the time of experimentation. Experimental procedures were approved by the Institutional Animal Care and Use Committees at the University of California, San Francisco and at Johns Hopkins University and were carried out in accordance with the guidelines on animal care and use of the US National Institutes of Health.

Viral vectors. For optogenetic conditioning experiments, Cre-dependent expression of channelrhodopsin was achieved via injection of AAV5-Ef1α-DIO-ChR2-eYFP (titer 1.5–4×10^{12} particles/ml, University of North Carolina) into the VTA or SNc. For projection-specific experiments, AAV2/5-Ef1α-hChR2(H134R)-eYFP-WPRE-hGH (1.5–4×10^{12} particles/ml, University of Pennsylvania), which exhibits retrograde transport[51], was injected into the NAc core or dorsal striatum. For combined optogenetic stimulation and photometry experiments, a mixture of AAVDJ-Ef1α-DIO-GCaMP6f (titer 1.0–3.9×10^{12}, Stanford University) and AAV9-hSyn-FLEX-ChrimsonR-tdTomato (1.5–4×10^{12} particles/ml, University of Pennsylvania) was injected into the VTA.

Surgical procedures. Viral infusions and optic fiber implants were carried out as previously described[52]. Rats were anesthetized with 5% isoflurane and placed in a stereotaxic frame, after which anesthesia was maintained at 1–3%. Rats were administered saline, carprofen anesthetic, and cefazolin antibiotic intraperitoneally. The top of the skull was exposed and holes were made for viral infusion needles, optic fiber implants, and five skull screws. Viral injections were made using a microsyringe pump at a rate of 0.1 μl/min. Injectors were left in place for 5 min, then raised 200 μm dorsal to the injection site, left in place for another 10 min, then removed slowly. Implants were secured to the skull with dental acrylic applied around skull screws and the base of the ferrule(s) containing the optic fiber. At the end of all surgeries, topical anesthetic and antibiotic ointment was applied to the surgical site, rats were removed to a heating pad and monitored until they were ambulatory. Rats were monitored daily for 1 week following surgery. Optogenetic manipulations commenced at least 4 weeks (6–8 weeks for photometry and projection-specific studies) after surgery.

Midbrain cell body targeting. AAV5-Ef1α-DIO-ChR2-eYFP was infused unilaterally (0.5 to 1 μl at each target site, for a total of 2–4 μl per rat) at the following coordinates from Bregma for targeting VTA cell bodies: posterior −6.2 and −5.4 mm, lateral +0.7, ventral −8.4 and −7.4. For targeting SNc dopamine cell bodies: posterior −5.8 and −5.0, lateral +2.4, ventral −8.0 and −7.0. Custom-made optic fiber implants (300-μm glass diameter) were inserted unilaterally just above and between viral injection sites at the following coordinates. VTA: posterior −5.8, lateral +0.7, ventral −7.5. SNc: posterior −5.3, lateral +2.4, ventral −7.3.

Projection-specific ChR2 targeting. The retrogradely-traveling AAV2/5-Ef1α-DIO-hChR2(H134R)-eYFP-WPRE-hGH was infused unilaterally into the NAc core, shell, or dorsal striatum. Two injections of 0.5 μl each (1 μl total per rat) were given along the anterior-posterior axis at these coordinates from Bregma. NAc core: anterior +2.2 and +1.6, lateral +1.6, ventral −7.0. NAc shell: anterior +1.8 and +1.2, lateral +0.75, ventral −7.5. Dorsal striatum: anterior +1.8 and +1.0, lateral +2.6, ventral −4.2. Optic fiber implants were inserted above the ipsilateral VTA (for NAc injections) or SNc (for dorsal striatal injections) at the coordinates listed above.

Photometry. A mixture of AAVDJ-Ef1α-DIO-GCaMP6f and AAV9-hSyn-FLEX-ChrimsonR-tdTomato (0.5–1 μl of each, for a total volume of 1–2 μl per rat) was injected into the VTA (posterior −5.8, lateral +0.7, ventral −8.0) or SNc (posterior −5.3, lateral +2.4, ventral −7.4). Low-auto-fluorescence optic fibers (400 μm, Doric) were inserted just dorsal to the injection site at the same coordinates as above.

Optogenetic stimulation. ChR2 studies used 473-nm lasers and ChrimsonR studies used 590-nm lasers (OptoEngine), adjusted to read ~10–20 mW from the end of the patch cable at constant illumination. Light output during individual 5-ms light pulses during experiments was estimated to be ~2 mW/mm² at the tip of the intracranial fiber. Light power was measured before and after every behavioral session to ensure that all equipment was functioning properly. For all optogenetic studies, optic tethers connecting rats to the rotary joint were sheathed in a lightweight armored jacket to prevent cable breakage and block visible light transmission.

Habituation and optogenetic Pavlovian training. Rats were first acclimated to the behavioral chambers (Med Associates), conditioning cues, and optic cable tethering in a ~30-min habituation session. During this session, rats were tethered to a rotary joint and 20 cue presentations, with no other consequences, were presented on a 90-s average variable time (VT) schedule. In each of 12 subsequent conditioning sessions, rats in paired groups were presented with 25 cue (light+tone, 7 s) – laser

stimulation (100 5-ms pulses at 20 Hz; laser train initiated 2 s after cue onset) pairings delivered on a 200-s VT schedule. These cues were never associated with another external stimulus (for example, food or water). Rats in unpaired groups also received 25 cue presentations and 25 laser trains per session, but an average 70-s VT schedule separated these events in time. The duration of laser stimulation was chosen to mimic the multi-second dopamine neuron activation we observed in vivo when these subjects consumed natural reward, such as sucrose (Supplementary Fig. 5). An additional group of rats was given the same optogenetic Pavlovian training procedure described above for paired groups, but each laser stimulation was only 1 s long (20 5-ms pulses at 20 Hz, Supplementary Fig. 4), delivered during the final second of each cue presentation. This group was included to confirm that brief dopamine neuron activation was sufficient to promote cue conditioned behavior. We also confirmed ex vivo that dopamine neurons could follow this stimulation pattern with light-evoked action potentials (Fig. 7 and Supplementary Fig. 9). In all groups, cue and laser delivery were never contingent on an animal's behavior and all rats received the same number of cue and laser events.

Conditioned Reinforcement. After optogenetic Pavlovian conditioning, rats were returned to the same behavioral chambers and tethered as before. At session onset, two levers were extended to the chamber below the cue lights used in the Pavlovian conditioning phase, and remained extended through the duration of the session. During 2 90-min sessions, presses on an active lever resulted in a 2-s presentation of the cue light-tone stimulus compound rats had received during Pavlovian training (fixed-ratio 1 schedule, with a timeout during each 2-s cue presentation), but no laser stimulation, to assess the conditioned reinforcing value of the cues alone. Inactive lever presses were recorded, but had no consequences.

Intracranial self-stimulation (2 1-h sessions). Rats were again returned to the behavioral chambers and tethered. During these sessions, nose poke ports were positioned on the wall opposite of the cue lights and levers from previous phases. During 2 1-h sessions, pokes in the active port resulted in a 1-s laser train (20 Hz, 20 5-ms pulses, fixed-ratio 1 schedule with a 1-s timeout during each train), but no other external cue events, to assess the reinforcing value of stimulation itself. Inactive nose pokes were recorded, but had no consequences.

Video scoring. Behavior during Pavlovian conditioning sessions was video recorded (Media Recorder 4.0, Noldus) using cameras positioned a standardized distance behind each chamber. Videos from sessions 1, 4, 8, and 12 were scored offline by observers who were blind to the identity and anatomical target group of the rats. Each cue (7 s, 25 per session) and laser (1 or 5 s, 25 per session) event was scored for the occurrence and onset latency of the following behaviors. Locomotion was defined as the rat moving all four feet in a forward direction (that is, not simply lifting feet in place). Cue approach was defined as the rat's nose coming within 1 in of the cue light (trials in which the rat's nose was in front of the light when it was presented were not counted in the approach measure). Approach often involved the rat moving from another area of the chamber to come in physical contact with the cue light while it was illuminated. Rearing was defined as the rat lifting its head and front feet off the chamber floor, either onto the side of the chamber, or into the air. Rotation was defined as the rat making a complete 360-degree turn in one direction.

Automated motion tracking and analysis. We supplemented experimenter scored video analysis with automated behavior tracking, to provide a detailed quantitative assessment of cue-evoked movement patterns. Behavioral videos from the final session of Pavlovian conditioning were analyzed using Noldus Ethovision XT software to automatically track the position of the rats' heads. The frame by frame location of the head within the video was transformed into a position coordinate within the experimental chamber. These coordinates were used to determine velocity (cm/s) and distance from the cue (cm) during pre-cue, cue, laser, and post-cue periods (Fig. 5 and Supplementary Fig. 8).

Ex vivo electrophysiology. 5–6 weeks following virus injection (described above), rats were deeply anesthetized with isoflurane, decapitated, and brains were removed. 200 μM horizontal slices of the midbrain were cut in ice cold aCSF, then maintained at 33 °C for current clamp recording as in previous studies[53]. ChR2-expressing neurons were identified with epiflourescence on the recording scope (AxioExaminer A1, also equipped with infrared and Dodt optics, Zeiss). ChR2 was activated by transmitting 470-nm light generated by an LED (XR-E XLamp LED; Cree) coupled to a 200-μm fiber optic pointed at the recorded cell and powered by an LED driver (Mightex Systems) and triggered by a Master 8. Cells were filled with biocytin during the recording, and when the recording was complete, the slice was fixed in 4% formaldehyde for 4 h. Immunocytochemistry was completed as in previous studies[53].

Fiber photometry. Fiber photometry allows for real-time excitation and detection of bulk fluorescence from genetically encoded calcium indicators, through the same optic fiber, in a freely moving animal. We first assessed dopamine neuron activity, via GCaMP6f fluorescence, in response to sucrose consumption, in order to determine the duration of activity during a reward exposure event, which we mimicked with optogenetic conditioning parameters. Rats underwent Pavlovian training wherein an auditory cue was presented on a 45-s variable time schedule.

VTA dopamine neurons in TH-Cre[+] rats ($n = 5$) were transfected with GCaMP6f and implanted with optic fibers for photometry. Rats first received magazine training during which sucrose was periodically delivered into a reward port. We then conducted photometry recordings during sessions where sucrose was delivered to the port on a 45-s VT schedule. We observed a rapid increase in fluorescence as animals consumed sucrose, lasting several seconds. These data show that natural reward consumption produces multi-second activation of dopamine neurons, at a comparable magnitude and duration, as measured by calcium fluorescence, to the 5-s laser stimulation train we employed in optogenetic conditioning studies (Supplementary Fig. 5).

To assess dopamine neuron activity during optogenetic Pavlovian conditioning, we co-transfected dopamine neurons with GCaMP6f and ChrimsonR, a red-shifted excitatory opsin[54]. This approach allowed for simultaneous measurement of activity-dependent fluorescence, excited by low power blue light, and optogenetic activation using orange light, in the same neurons[55]. The photometry system was constructed similar to previous studies[40]. A fluorescence mini-cube (Doric Lenses) transmitted light streams from a 465-nm LED sinusoidally modulated at 211 Hz that passed through a GFP excitation filter, and a 405-nm LED modulated at 531 Hz that passed through a 405-nm bandpass filter. LED power was set at ~100 µW. The mini-cube also transmitted light from a 590-nm laser, for optogenetic activation of ChrimsonR through the same low-autofluorescence fiber cable (400 nm, 0.48 NA), which was connected to the optic fiber implant on the rat. GCaMP6f fluorescence from neurons below the fiber tip in the brain was transmitted via this same cable back to the mini-cube, where it was passed through a GFP emission filter, amplified, and focused onto a high sensitivity photoreceiver (Newport, Model 2151). Demodulation of the brightness produced by the 465-nm excitation, which stimulates calcium-dependent GCaMP6f fluorescence, versus isosbestic 405-nm excitation, which stimulates GCaMP6f in a calcium-independent manner, allowed for correction for bleaching and movement artifacts. A real-time signal processor (RP2.1, Tucker-Davis Technologies) running OpenEx software modulated the output of each LED and recorded photometry signals, which were sampled from the photodetector at 6.1 kHz. The signals generated by the two LEDs were demodulated and decimated to 382 Hz for recording to disk. For analysis, both signals were then downsampled to 40 Hz, and a least-squares linear fit was applied to the 405-nm signal, to align it to the 465-nm signal. This fitted 405-nm signal was used to normalize the 465-nm signal, where $\Delta F/F = $ (465-nm signal – fitted 405-nm signal)/(fitted 405-nm signal). Task events (for example, cue and laser presentations) were time stamped in the photometry data file via a signal from the Med-PC behavioral program, and behavior was video recorded as described above.

Photometry rats (Cue Paired group, $n = 8$) underwent opto-Pavlovian conditioning, similar to that described above, but the intertrial interval for these experiments was halved to 100-s VT, for a ~40-min session length. This was done to shorten the overall length of photometry measurement periods to minimize photobleaching of GCaMP-expressing cells. Photometry measurements were made on training sessions 1, 4, 8, and 12, during which both LED channels were modulated continuously, as described above. On these 4 sessions, 20% of trials (5/25), pseudo-randomly presented, were 'probes', where cues were presented without accompanying optogenetic stimulation. Unpaired rats ($n = 5$) received 12 sessions of cue and laser presentations (25 each) separated by a 70-s VT.

Following conditioning, a subset of paired animals ($n = 5$) received one session of extinction training, during which cues were presented as before, but laser was omitted, while photometry measurements were made.

For baseline characterization of ChrimsonR-activated GCaMP6f signals, rats ($n = 5$) were tethered to the photometry apparatus, and continuous photometry measurements were made during a series of 60 unsignaled 590-nm laser presentations (30 trials of 1-s, 20 Hz stimulation trains, 30 trials of 5-s, 20 Hz trains, counterbalanced), delivered on a 30-s VT schedule.

ChrimsonR ICSS. Th-Cre[+] rats ($n = 7$) were given the opportunity to respond for 590-nm laser pulses (1 s, 20 Hz), in 2 1-h sessions, similar to above, to validate ChrimsonR support of dopamine-mediated primary reinforcement. On a third session, the laser was switched from orange to blue (473 nm), to verify that ChrimsonR activation necessary to support behavior is specific to red-shifted light.

Statistics, data collection, and analysis. Rats were randomly assigned to conditioning groups (paired, unpaired) following surgery. Behavioral data from optogenetic conditioning experiments was automatically recorded with Med-PC software (Med Associates) and analyzed using Prism 6.0. Video of conditioning sessions was recorded using Noldus Media Recorder 4.0, and automated behavior tracking data was generated using Noldus Ethovision XT and analyzed in MATLAB. For manual video scoring, experimenters were blind to the anatomical and conditioning group identity. Experimenters were otherwise not blinded. Non-parametric tests were used when data distributions were non-normal. Two-way repeated measures ANOVA was used to analyze changes in behavior among the groups across training. Bonferroni-corrected post hoc comparisons were made to compare groups on individual sessions. No statistical tests were used to predetermine sample sizes, but our sample sizes were similar to previously published studies. Rats were included in optogenetic behavioral analyses if optic

fiber tips were no more than ~500 µm dorsal to the target region (VTA or SNc). Photometry data were collected with TDT OpenEx and Synapse software and analyzed using MATLAB. To assess the change in fluorescence across training days we fit a linear mixed-effect model for $\Delta F/F$ during each period of interest (0–1 s post-cue and laser omission period), with fixed effects for day and random effects for subject. To assess the relationship between the magnitude of cue-evoked fluorescence and CR latency, we fit a linear mixed-effect model for latency with fixed effects for cue-evoked fluorescence magnitude and random effects for subject. All comparisons were two tailed. Data in figures are expressed as the mean ± s.e.m. Statistical significance was set at $P < 0.05$. Please see the Nature Research Reporting Summary for additional information.

Histology. Rats were deeply anesthetized with sodium pentobarbital and transcardially perfused with cold phosphate buffered saline followed by 4% paraformaldehyde. Brains were removed and post-fixed in 4% paraformaldehyde for ~24 h, then cryoprotected in a 25% sucrose solution for at least 48 h. Sections were cut at 50 µm on a cryostat (Leica Microsystems). To confirm viral expression and optic fiber placements, brain sections containing the midbrain were mounted on microscope slides and coverslipped with Vectashield containing DAPI counterstain. Fluorescence from ChR2-eYFP and ChrimsonR-tdTomato as well as optic fiber damage location was then visualized. Tissue from Cre[–] animals was examined for lack of viral expression and optic fiber placements. To verify localization of viral expression in dopamine neurons we performed immunohistochemistry for tyrosine hydroxylase and GFP/tdTomato. Sections were washed in PBS and incubated with bovine serum albumin (BSA) and Triton X-100 (each 0.2%) for 20 min. 10% normal donkey serum (NDS) was added for a 30-min incubation, before primary antibody incubation (mouse anti-GFP, 1:1,500, Invitrogen; rabbit anti-TH, 1:500, Fisher Scientific) overnight at 4 °C in PBS with BSA and Triton X-100 (each 0.2%). Sections were then washed and incubated with 2% NDS in PBS for 10 min and secondary antibodies were added (1:200 Alexa Fluor 488 donkey anti-mouse, 594 donkey anti-rabbit or 647 chicken anti-rabbit) for 2 h at room temperature. Sections were washed twice in PBS and mounted with Vectashield containing DAPI. Brain sections were imaged with a Zeiss Axio 2 microscope.

For cell counting to quantify targeting specificity in TH-Cre rats (Supplementary Fig. 1), the Apotome microscope function was used to take 20× three-channel images along the medial-lateral and anterior-posterior gradients of the midbrain, using equivalent exposure and threshold settings. With the TH channel turned off, YFP^{+} cells were first identified by a clear ring around DAPI-stained nuclei. The TH channel was then overlaid, and the proportion of YFP^{+} cells coexpressing TH was counted. Cell counting for quantification of ChrimsonR and GCaMP6f expression overlap (Supplementary Fig. 5) was done as above. GCaMP6f^{+}, ChrimsonR[+], and TH^{+} cells directly below optic fiber placements were counted to determine the overlap of these three markers.

For assessing retrograde AAV expression (Supplementary Fig. 10), sections containing the striatum and midbrain from brains with AAV2/5-Ef1α-DIO-hChR2(H134R)-eYFP-WPRE-hGH injections targeting the NAc core ($n = 4$), shell ($n = 5$), or dorsal striatum ($n = 5$) were processed with immunohistochemistry for YFP and TH, as above. Tiled images of whole sections (6–10 sections per rat) containing the midbrain were then taken at three approximate anatomical levels: –5.0, –5.5, and –6.0 mm posterior to bregma based on the Paxinos and Watson rat brain atlas. The topography of retrograde expression was estimated by drawing regions of interest (ROIs) around the area within each brain section containing YFP[+] cell bodies. Individual brain slices containing these ROIs were then overlaid in Adobe Illustrator and aligned to standardized atlas plates for visualization of average expression patterns according to projection.

Reporting Summary. Further information on experimental design is available in the Nature Research Reporting Summary linked to this article.

Data and code availability. The data supporting these findings are available from the corresponding authors upon request. All MATLAB code used in analysis of these findings is available from the corresponding authors upon request.

References

51. Rothermel, M., Brunert, D., Zabawa, C., Díaz-Quesada, M. & Wachowiak, M. Transgene expression in target-defined neuron populations mediated by retrograde infection with adeno-associated viral vectors. *J. Neurosci.* **33**, 15195–15206 (2013).

52. Steinberg, E. E. et al. Positive reinforcement mediated by midbrain dopamine neurons requires D1 and D2 receptor activation in the nucleus accumbens. *PLoS One* **9**, e94771 (2014).

53. Margolis, E. B., Hjelmstad, G. O., Fujita, W. & Fields, H. L. Direct bidirectional µ-opioid control of midbrain dopamine neurons. *J. Neurosci.* **34**, 14707–14716 (2014).

54. Klapoetke, N. C. et al. Independent optical excitation of distinct neural populations. *Nat. Methods* **11**, 338–346 (2014).

55. Kim, C. K. et al. Simultaneous fast measurement of circuit dynamics at multiple sites across the mammalian brain. *Nat. Methods* **13**, 325–328 (2016).

naturereasearch

Corresponding author(s):   Benjamin Saunders and Patricia Janak

Reporting Summary

Nature Research wishes to improve the reproducibility of the work that we publish. This form provides structure for consistency and transparency in reporting. For further information on Nature Research policies, see Authors & Referees and the Editorial Policy Checklist.

Statistical parameters

When statistical analyses are reported, confirm that the following items are present in the relevant location (e.g. figure legend, table legend, main text, or Methods section).

n/a	Confirmed	
☐	☒	The exact sample size (*n*) for each experimental group/condition, given as a discrete number and unit of measurement
☐	☒	An indication of whether measurements were taken from distinct samples or whether the same sample was measured repeatedly
☐	☒	The statistical test(s) used AND whether they are one- or two-sided *Only common tests should be described solely by name; describe more complex techniques in the Methods section.*
☐	☒	A description of all covariates tested
☐	☒	A description of any assumptions or corrections, such as tests of normality and adjustment for multiple comparisons
☐	☒	A full description of the statistics including central tendency (e.g. means) or other basic estimates (e.g. regression coefficient) AND variation (e.g. standard deviation) or associated estimates of uncertainty (e.g. confidence intervals)
☐	☒	For null hypothesis testing, the test statistic (e.g. *F*, *t*, *r*) with confidence intervals, effect sizes, degrees of freedom and *P* value noted *Give P values as exact values whenever suitable.*
☒	☐	For Bayesian analysis, information on the choice of priors and Markov chain Monte Carlo settings
☒	☐	For hierarchical and complex designs, identification of the appropriate level for tests and full reporting of outcomes
☐	☒	Estimates of effect sizes (e.g. Cohen's *d*, Pearson's *r*), indicating how they were calculated
☐	☒	Clearly defined error bars *State explicitly what error bars represent (e.g. SD, SE, CI)*

Our web collection on statistics for biologists may be useful.

Software and code

Policy information about availability of computer code

Data collection	Data were collected with readily available software (Med-PC 4.0, Tucker Davis Synapse 2.0 and Ethovision XT 10)
Data analysis	Data were analyzed with Prism 6.0 and MATLAB 2017b. Adobe Illustrator CC 2017 was used in the production of data figures.

For manuscripts utilizing custom algorithms or software that are central to the research but not yet described in published literature, software must be made available to editors/reviewers upon request. We strongly encourage code deposition in a community repository (e.g. GitHub). See the Nature Research guidelines for submitting code & software for further information.

Data

Policy information about availability of data

All manuscripts must include a data availability statement. This statement should provide the following information, where applicable:

- Accession codes, unique identifiers, or web links for publicly available datasets
- A list of figures that have associated raw data
- A description of any restrictions on data availability

Data are available upon request to the corresponding authors.

Field-specific reporting

Please select the best fit for your research. If you are not sure, read the appropriate sections before making your selection.

☒ Life sciences ☐ Behavioural & social sciences ☐ Ecological, evolutionary & environmental sciences

For a reference copy of the document with all sections, see nature.com/authors/policies/ReportingSummary-flat.pdf

Life sciences study design

All studies must disclose on these points even when the disclosure is negative.

Sample size	Sample size was not statistically predetermined, but based on common practice in these types of research studies, and practical issues with respect to in vivo measurement techniques.
Data exclusions	A small number of animals were excluded (n=6) because optic fiber placements were not over the area of viral expression.
Replication	Results were serially replicated through multiple cohorts.
Randomization	Animals were randomly assigned to anatomical groups at the time of surgery, and randomly assigned to conditioning groups before the start of experiments.
Blinding	Investigators were blind to subject group for analyses.

Reporting for specific materials, systems and methods

Materials & experimental systems

n/a	Involved in the study
☒	☐ Unique biological materials
☐	☒ Antibodies
☒	☐ Eukaryotic cell lines
☒	☐ Palaeontology
☐	☒ Animals and other organisms
☒	☐ Human research participants

Methods

n/a	Involved in the study
☒	☐ ChIP-seq
☒	☐ Flow cytometry
☒	☐ MRI-based neuroimaging

Antibodies

Antibodies used	Rabbit anti-tyrosine hydroxylase, 1:500, Fisher Scientific, #OPA1-04050 Mouse anti-GFP, 1:1500, Fisher Scientific, #A11120 Alexa Fluor 488 donkey anti-mouse, Life Technologies, #R37114 Alexa Fluor 594 donkey anti-rabbit, Life Technologies, #R37119 Alexa Fluor 647 chicken anti-rabbit, Life Technologies, #A21443
Validation	The specificity of the TH and GFP antibodies was validated by the manufacturer, and in previous publications (PMID: 25451178, PMID: 21515375, PMID: 26916822, PMID: 24569479. In addition, we observed TH and GFP staining specifically in cell bodies in the VTA and SNc, and in terminals in the striatum in TH-cre positive, but not TH-cre negative animals, which serves as an anatomical-based control for these antibodies. TH or GFP fluorescence was not seen in brain regions what do not contain TH+ neurons. Specificity of the secondary antibodies was confirmed by verifying a lack of expression in tissue sections in which the primary antibody was omitted from the immunohistochemical protocol.

Animals and other organisms

Policy information about studies involving animals; ARRIVE guidelines recommended for reporting animal research

Laboratory animals	Male and female TH-cre transgenic rats (from a Long Evans background; Witten et al., Neuron, 2011) were used, derived from an in house breeding colony. Animals were at least 3 months old at the onset of surgical procedures.
Wild animals	Wild animals were not used.

| Field-collected samples | Field samples were not collected. |